

Pore-Filling of Spiro-OMeTAD in Solid-State Dye Sensitized Solar Cells: Quantification, Mechanism, and Consequences for Device Performance

By I-Kang Ding, Nicolas Tétreault, Jérémie Brillet, Brian E. Hardin, Eva H. Smith, Samuel J. Rosenthal, Frédéric Sauvage, Michael Grätzel, and Michael D. McGehee*

In this paper, the pore filling of spiro-OMeTAD (2,2',7,7'-tetrakis-(*N,N*-di-*p*-methoxyphenylamine)9,9'-spirobifluorene) in mesoporous TiO₂ films is quantified for the first time using XPS depth profiling and UV–Vis absorption spectroscopy. It is shown that spiro-OMeTAD can penetrate the entire depth of the film, and its concentration is constant throughout the film. We determine that in a 2.5- μm -thick film, the volume of the pores is 60–65% filled. The pores become less filled when thicker films are used. Such filling fraction is much higher than the solution concentration because the excess solution on top of the film can act as a reservoir during the spin coating process. Lastly, we demonstrate that by using a lower spin coating speed and higher spiro-OMeTAD solution concentration, we can increase the filling fraction and consequently the efficiency of the device.

1. Introduction

Dye-sensitized solar cells (DSCs) are one of the most promising photovoltaic technologies. Liquid electrolyte-based DSCs have reached efficiencies as high as 11.1%.^[1–3] However, these liquid-based DSCs suffer from potential leakage and corrosion problems;^[4] these disadvantages have sparked research in solid-state dye-sensitized solar cells (ss-DSCs), which have solid-state hole transport materials (HTMs) instead of liquid electrolytes. One of the most widely-used HTMs is spiro-OMeTAD (2,2',7,7'-tetrakis-(*N,N*-di-*p*-methoxyphenylamine)9,9'-spirobifluorene).^[5] ss-DSCs with spiro-OMeTAD as HTM have attained efficiencies exceeding 5%,^[6] which is still far below the efficiency of liquid electrolyte DSCs. The lower efficiency is primarily a consequence of incomplete light harvesting. The highest-performing ss-DSCs

to date have a 2 μm thick active layer,^[7] far thinner than the thickness needed to achieve good optical absorption. There are two factors that limit the ss-DSCs from being more efficient at thicknesses $>2 \mu\text{m}$: electron–hole recombination and incomplete filling of the mesoporous TiO₂ films with spiro-OMeTAD. Studies on recombination show that recombination in ss-DSCs is two orders of magnitude faster than in liquid DSCs^[8] and the electron diffusion length (L_D) in mesoporous TiO₂ is 6–12 μm , much larger than the optimized 2- μm film thickness.^[9–11] A recent study has shown that reducing the recombination rate constant by using ion-coordinating ruthenium dyes did not increase the

optimum solar cell thickness.^[6] This finding led the scientific community to conclude that recombination may not be the only factor limiting device thickness, and that in order to improve device efficiency, understanding pore filling is crucial. Few studies have attempted to characterize the pore filling in ss-DSCs made with spiro-OMeTAD, and the techniques used have been limited to qualitative analysis. Schmidt-Mende et. al. used cross-section scanning electron microscopy (SEM) to qualitatively compare the pore filling between three different HTMs.^[12] Kroeze et. al. used transient absorption and reported that spiro-OMeTAD could infiltrate to the bottom of 2- μm -thick films. Furthermore, they showed that in such spiro-OMeTAD-infiltrated films, almost all the dye cations can transfer holes to spiro-OMeTAD, indicating that the spiro-OMeTAD is capable of wetting pores of all sizes.^[13]

The infiltration depth and the filling fraction (i.e., volume fraction of the pores filled by the HTM) are important parameters of pore filling. Shallow infiltration depth of spiro-OMeTAD prevents dye molecules in the bottom of the film from transferring holes to spiro-OMeTAD and contributing to photocurrent. The filling fraction corresponding to monolayer coverage of spiro-OMeTAD inside pores is calculated with the molecule size (2 nm)^[14] and pore diameter (20 nm)^[15] to be 49%. Low filling fraction (<49%) leads to increased recombination and series resistance.

Infiltration of spiro-OMeTAD into mesoporous TiO₂ film is usually accomplished by depositing spiro-OMeTAD solution on the film and soaking the film for 1 minute, followed by spin coating to remove excess solution. Prior to spin coating, the pores are filled

[*] Prof. M. D. McGehee, I.-K. Ding, B. E. Hardin, E. H. Smith, S. J. Rosenthal
Department of Materials Science and Engineering
Stanford University
Stanford, CA 94305 (USA)
E-mail: mmcgehee@stanford.edu
Dr. N. Tétreault, J. Brillet, F. Sauvage, Prof. M. Grätzel
Institut de Chimie Physique
École Polytechnique Fédérale de Lausanne
1015 Lausanne (Switzerland)

DOI: 10.1002/adfm.200900541

with solution effectively by capillary action. If no further infiltration takes place during spin coating, the filling fraction should be 10% (equal to volumetric concentration of solution). Such filling fraction is much lower than the 49% required to form monolayer inside pores, and also lower than the 20% filling fraction for ss-DSCs made with poly(3,4-ethylenedioxythiophene) (PEDOT)^[16] and 100% filling fraction for ss-DSCs made with CuSCN.^[17] Snaith et. al. have proposed that in the spiro-OMeTAD system, the filling fraction is much higher than the solution concentration because the excess solution on top of the film can act as a reservoir during the spin coating process.^[18] As the solvent evaporates, the concentration of spiro-OMeTAD in the reservoir increases and more spiro-OMeTAD diffuses into the pores. Furthermore, the filling fraction of spiro-OMeTAD was calculated from overlayer thickness through the following equation:

$$F = c + (c \cdot t_{\text{WET}} - t_{\text{OL}}) / (t_{\text{TiO}_2} \times p) \quad (1)$$

where F is the filling fraction, c is the volume ratio of spiro-OMeTAD in solution (10% for 180 mg mL⁻¹ solution), t_{WET} is the wet reservoir thickness in spin-coating process, t_{OL} is the spiro-OMeTAD overlayer thickness, t_{TiO_2} is the TiO₂ film thickness, and p is the film porosity. The t_{WET} is assumed to be the same as the spin coated film on a dye-modified, flat TiO₂ layer. Figure 1 illustrates the pore filling process and the definition of parameters used in Equation 1. To date Equation 1 has not been experimentally verified.

In this paper, we present the first quantification of spiro-OMeTAD pore filling in mesoporous TiO₂ films. Using X-ray photoelectron spectroscopy (XPS) depth profiling, we show that spiro-OMeTAD can infiltrate all the way to the bottom of 5- μm -thick films, and its concentration is constant throughout the film. From UV-vis absorption spectroscopy, we determine that in a state-of-art device with 2.5- μm thickness, the volume of the pores is 60–65% filled. However, the filling fraction is lower for thicker films. We find that Equation 1 correctly predicts how filling fraction depends on film thickness. Based on our findings, we conclude that the filling fraction is inherently limited by the quantity of spiro-OMeTAD that can infiltrate into the pores before the excess solution is either depleted or dried. We show that using either higher spiro-OMeTAD concentration in chlorobenzene or a slower spinning speed increases the filling fraction and the power conversion efficiency of ss-DSCs. Increasing the concentration in solution improves the efficiency of 2.4- μm - and 3.0- μm -thick ss-DSCs by about 20% to 4.05% and 50% to 3.18%, respectively. Similarly, decreasing the spinning speed from 2 000 RPM to 600 RPM increases the efficiency of 3.0- μm -thick ss-DSCs by about 60% to 3.53%, while leaving the efficiency of thinner films unaffected.

2. Results and Discussion

2.1. X-ray Photoelectron Spectroscopy: Determining Depth Profile

XPS depth profiling provides the most quantitative data for depth profiling the spiro-OMeTAD inside films compared to other characterization techniques. Scanning electron microscopy with energy dispersive spectrometry (SEM-EDS) has been employed on the cross section of ss-DSCs made with polymer-based electro-

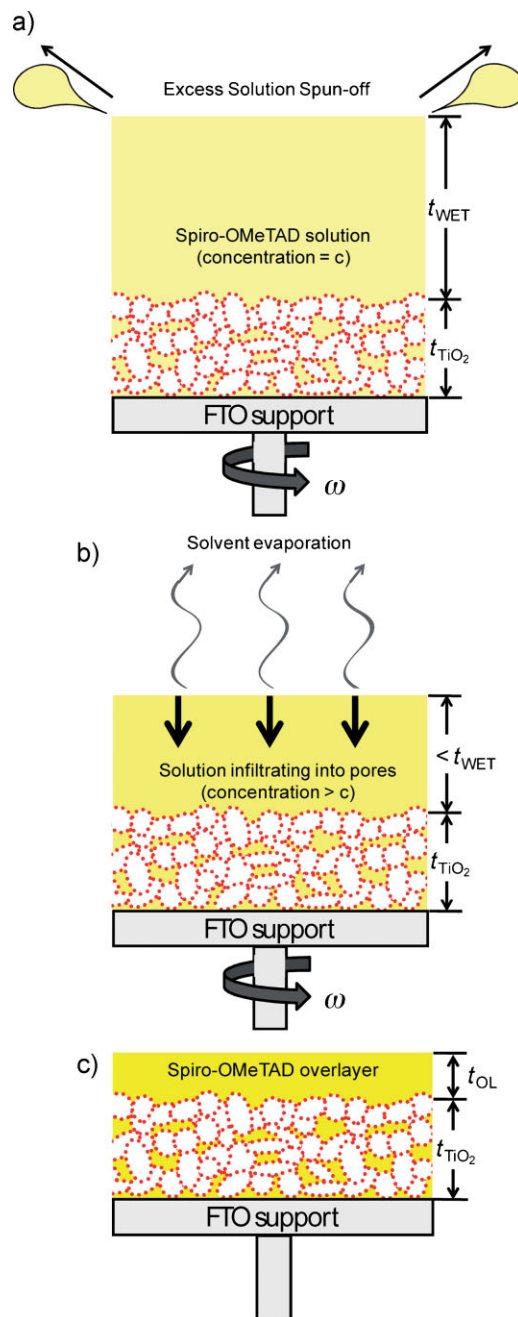


Figure 1. Schematic illustration of pore filling process during spin-coating. The process can be divided into three stages. a) At the very beginning of spin coating, the excess spiro-OMeTAD solution on top of the TiO₂ film (thickness = t_{WET}) can act as a reservoir. b) During spin coating, this reservoir increases the filling fraction beyond the solution concentration until it completely infiltrates into the film or dries on top. c) After spin coating, the spiro-OMeTAD that did not infiltrate into the pores stay on top of the TiO₂ film as dry overlayer (thickness = t_{OL}).

lytes,^[19] but this technique has poor spatial resolution (1 μm) and limited quantitative ability. Auger electron spectroscopy (AES) has adequate spatial resolution to scan the cross section of the films, but because organic materials are mechanically weaker than TiO₂, the cross section can be composed entirely of spiro-OMeTAD.^[20]

Consequently, the composition in the cross section can be very carbon-rich and deviate greatly from the real composition. Our AES measurements on spiro-OMeTAD-infiltrated TiO_2 films showed a filling fraction higher than unity (see Supporting Information); therefore, we concluded that AES was not suitable for this purpose. Secondary ion mass spectroscopy (SIMS) has good depth resolution; however, the sensitivity factor for each element is strongly dependent on the matrix and can vary by as much as four orders of magnitude.^[21] Therefore, standards such as carbon-implanted TiO_2 are necessary in order to perform accurate quantification. Because the standards for this particular system have not been established, the quantitative ability of SIMS is limited. X-ray photoelectron spectroscopy (XPS) depth profiling is the most suitable technique to probe the concentration versus depth as it has very good depth resolution and quantitative ability. It has been used to characterize the depth profile of other organic materials in an inorganic matrix.^[22,23]

The XPS depth profiles of spiro-OMeTAD-infiltrated mesoporous TiO_2 films are shown in Figure 2. The 5- μm -thick mesoporous films have three different particle sizes and were prepared by doctor-blading. The contribution of the carbon signal from the Z907 dye molecule was quantified by the Ruthenium 3d5 peak and subtracted (see Supporting Information), so the carbon signal intensity reflected only the spiro-OMeTAD concentration inside the film. We observed that for all three particle sizes studied, spiro-OMeTAD can infiltrate all the way to the bottom of 5- μm -thick film. This finding indicates that the optimum device thickness (2 μm) is not limited by the infiltration depth of the HTM. Furthermore, the carbon concentration is constant throughout the film, indicating the absence of a spiro-OMeTAD concentration gradient. This phenomenon was also observed for spiro-OMeTAD-infiltrated samples without Z907 modification. After spin coating, some chlorobenzene remains inside the pores, allowing spiro-OMeTAD to diffuse and resulting in the constant spiro-OMeTAD concentration profile. The presence of undried chlorobenzene inside the pores is confirmed by the $\sim 20\text{-}\mu\text{g}$ weight loss (which corresponds to 20–40% of pore volume) over the course of one day after spin coating.

Unfortunately, XPS could not be used to determine the absolute ratio of one element to another because organic compounds (i.e., spiro-OMeTAD) sputter away faster than TiO_2 , causing the surface composition to deviate from the bulk volumetric composition. Such a “preferential sputtering” phenomenon is evident from the observation that elemental composition ratio changes with the accelerating voltage of the ion beam. For the sample with 20-nm TiO_2 particles (Fig. 2b), the average C/Ti ratio increased from 0.32 to 0.76 when the accelerating voltage of Argon-ion sputter beam was reduced from 5 kV to 500 V. Although the preferential sputtering prevents us from using the XPS data to determine the filling fraction, it does not undermine the accuracy of the relative concentration gradient in depth profile. This is because the TiO_2 and spiro-OMeTAD phases are intermixed, and the sputter beam cannot remove spiro-OMeTAD faster than the TiO_2 once the system reaches equilibrium with a Ti-rich surface.

2.2. Absorption Spectroscopy: Measuring Filling Fraction

We used absorption spectroscopy to quantify the volume fraction of pores filled by spiro-OMeTAD. We immersed the sample in a known volume of chlorobenzene for one hour to dissolve the spiro-

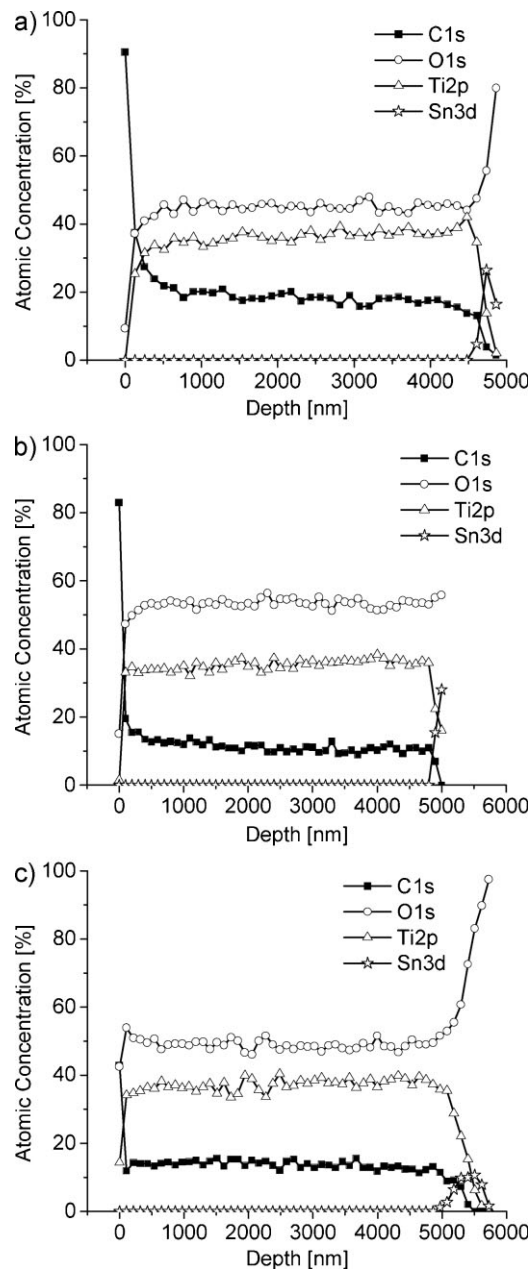


Figure 2. XPS depth profiling of spiro-OMeTAD infiltrated in mesoporous TiO_2 films made with different particle sizes. The zero depth corresponds to the air- TiO_2 interface. a) 9-nm nanoparticles (NPs) on FTO; b) 20-nm NPs on FTO; c) 37-nm NPs on FTO. The peaks used to detect elemental concentration were carbon 1s (filled squares), oxygen 1s (outlined circles), titanium 2p (outlined triangles), and tin 3d (outlined stars). The carbon contribution from the adsorbed Z907 dye has been subtracted.

OMeTAD out from the pores, and determined the concentration by measuring the absorption in the solution phase. The complete removal of spiro-OMeTAD through solvent immersion was confirmed by XPS depth profiling. After immersion, the resulting mesoporous TiO_2 film showed virtually no carbon signal from spiro-OMeTAD. We chose not to measure absorption in the film itself because mesoporous TiO_2 films scatter strongly for $\lambda < 400\text{ nm}$, and light scattering would complicate the absorption measurement.

In calculating the filling fraction through absorption, we used the following parameters: spiro-OMeTAD molar extinction coefficient in chlorobenzene = $7.47 \times 10^4 \text{ M}^{-1} \text{ cm}^{-1}$ ($\lambda_{\text{max}} = 389 \text{ nm}$), porosity of TiO_2 film without ruthenium dye modification = 0.68 (measured with the Brunauer, Emmett, and Teller (BET) method), porosity shrinkage for films of 20-nm TiO_2 particles due to ruthenium dye modification = 30%,^[24] and spiro-OMeTAD density = 1.82 g cm^{-3} (see Supporting Information). The filling fraction is calculated by dividing the volume of spiro-OMeTAD by the volume of pores. For 2.8- μm -thick TiO_2 films infiltrated with spiro-OMeTAD through literature-reported procedures (solution concentration = 180 mg mL^{-1} , soak time = 1 min, spin coating speed = 2000 RPM),^[25] the filling fraction was $\sim 60\text{--}65\%$. This is lower than the 85% filling fraction suggested by Snaith et. al.,^[18] but much higher than the solution concentration (10% of spiro-OMeTAD by volume). It should be noted that the filling fraction was the same for samples with and without Z907 dye modification, underlining the importance of the capillary-based infiltration mechanism.

The filling fraction as a function of spiro-OMeTAD solution concentration was measured for three different TiO_2 film thicknesses, shown in Figure 3a. For each solution concentration, we measured the overlayer thickness with SEM cross-section and subsequently calculated the wet reservoir thickness, t_{WET} , from the filling fraction of the 2.8- μm samples. For the samples prepared

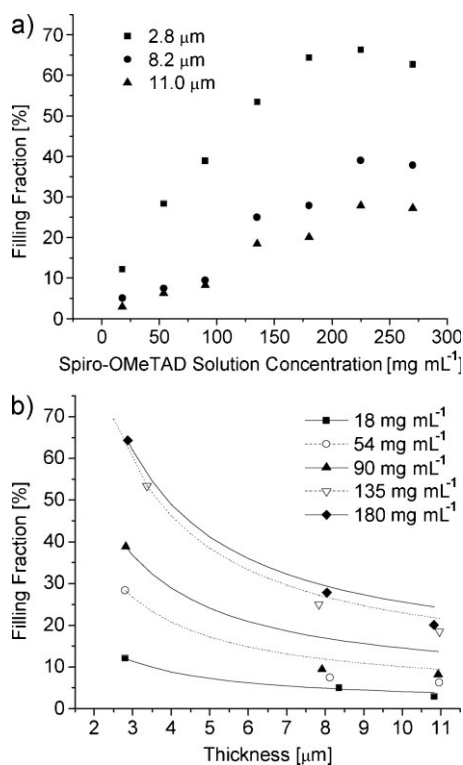


Figure 3. a) Filling fraction as a function of solution concentration for three different TiO_2 film thicknesses: 2.8 μm (squares), 8.2 μm (circles), and 11.0 μm (triangles). b) Filling fraction as a function of film thicknesses for five different solution concentrations: 18 mg mL^{-1} (filled squares), 54 mg mL^{-1} (outlined circles), 90 mg mL^{-1} (filled triangles), 135 mg mL^{-1} (outlined inverted triangles), and 180 mg mL^{-1} (filled diamonds). The lines are the curve fits with Equation 1 for different solution concentrations.

with solution concentration of 180 mg mL^{-1} , the dry reservoir thickness ($c \cdot t_{\text{WET}}$) is around 0.7 μm . The dry reservoir thickness is different from the dry spiro-OMeTAD layer thickness, as determined by spin coating the solution on a dye-coated compact TiO_2 film, indicating the spin coating conditions on a flat substrate and on a mesoporous film are different. Subsequently, the calculated reservoir thickness, t_{WET} , was used to fit filling fraction as a function of film thickness, shown in Figure 3b. Our results closely match the predicted filling fraction using Equation 1, which validates the reservoir model proposed by Snaith et. al.^[18] For thicker TiO_2 films the filling fraction was $\sim 20\text{--}40\%$, indicating submonolayer coverage of spiro-OMeTAD. Such incomplete coverage likely causes an increase in recombination and series resistance,^[8] and limits the number of dye molecules that can transfer holes to spiro. These issues may be responsible for the lower efficiency of thicker devices.

Figure 3a shows that the filling fraction is proportional to the solution concentration up to 225 mg mL^{-1} for 2.8- μm films and 275 mg mL^{-1} for 8.2- μm films. When the concentration is increased further, spiro-OMeTAD overlayers begin to appear on top of TiO_2 film and the filling fraction saturates. This indicates that, during spin coating, the excess solution on top of the film infiltrates into the pores while solvent evaporates. The infiltration process stops when enough solvent has evaporated for the spiro-OMeTAD molecules to become immobile. Therefore, the maximum filling fraction is limited kinetically by the quantity of spiro-OMeTAD that can infiltrate into the pores before the critical solution concentration is reached.

Based on our findings, the thickness of the ss-DSCs is not limited by the infiltration depth of spiro-OMeTAD, but may be limited by the lower filling fraction of thick films and concomitant electron-hole recombination. Increasing the filling fraction may slow recombination by increasing the separation distance between holes in spiro-OMeTAD and electrons in TiO_2 . In order to increase the size of the reservoir during pore filling and thereby increase the filling fraction, we increased the solution concentration (Fig. 3a) and decreased the spin coating speed (Fig. 4). Both approaches are shown to be effective in increasing the filling fraction. However, these approaches also lead to undesirable increase in the overlayer thickness, which will increase the series resistance.

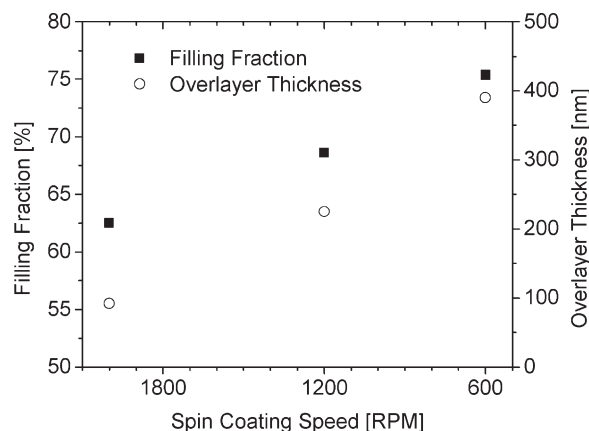


Figure 4. Filling fraction (filled squares) and spiro-OMeTAD overlayer thickness (outlined circles) in 2.8- μm -thick TiO_2 films as a function of spin coating speed. The spiro-OMeTAD solution concentration is 180 mg mL^{-1} .

2.3. Influence of Filling Fraction on Solar Cell Performance

We examined how filling fraction affects device performance. Figure 5a presents the energy conversion efficiency for 2.4- μm and 3.0- μm solar cells made with spiro-OMeTAD concentrations in the 130 to 275 mg mL^{-1} range. In general, the ss-DSC efficiency increases with increasing filling fraction up to a spiro-OMeTAD concentration of 225 mg mL^{-1} for 2.4- μm -thick cells and up to 275 mg mL^{-1} for 3.0- μm -thick cells. While the open-circuit voltage (V_{oc}) stays constant for all cells, the short-circuit current (J_{sc}) and fill factor are optimal at 225 mg mL^{-1} of spiro-OMeTAD in chlorobenzene for the thinner, 2.4- μm , ss-DSCs. At higher concentration, the increasing overlayer thickness adds to the series resistance and causes the fill factor to decrease by more than 20%.^[26] Overall, the efficiency of the 2.4- μm -thick ss-DSC increases by about 20% from 3.38% to 4.05% at 225 mg mL^{-1} of spiro-OMeTAD in chlorobenzene. In accordance with the reservoir theory, the fill factor for the thicker, 3.0- μm , ss-DSC is higher than for thinner films at all concentrations, confirming that more of the reservoir's spiro-OMeTAD infiltrated the pores and left a thinner overlayer. This leads to a 50% increase in the efficiency from 2.12% to 3.18% due to the current density increasing with filling fraction and a sustained fill factor even at 275 mg mL^{-1} of spiro-OMeTAD in chlorobenzene.

Figure 5b shows the power conversion efficiency as the spin coating speed is decreased from 2000 RPM to 600 RPM. In general, the decreased spin coating speed has a negligible effect on 2.4- μm or thinner ss-DSCs. However, for 3.0- μm -thick ss-DSCs, there is a direct correlation between the increase in filling fraction and an enhanced photocurrent when slowing down the spinning

speed from 2000 RPM to 600 RPM. Since the overlayer thickness stays low and, hence, the fill factor stays unchanged, the higher current density increases the overall energy conversion efficiency by about 60%, from 2.21% to 3.53%.

These results show that increasing the filling fraction by increasing the HTM concentration in solution or decreasing the spin coating speed is a good strategy to increase the photocurrent in ss-DSCs. However, both of the techniques used in this study also increase the overlayer thickness and adversely affect the fill factor. Therefore, a compromise between higher filling fraction and a thicker overlayer must be found. Additionally, it is evident from this study that the optimal compromise is dependent on the thickness of TiO_2 film. Work to reduce the recombination by enhancing pore filling or by passivating the TiO_2 surface with a wide bandgap oxide^[27] is currently in progress.

3. Conclusions

We have developed procedures to measure pore filling quantitatively using XPS depth profiling and absorption spectroscopy. We found that solution infiltration of spiro-OMeTAD in mesoporous TiO_2 films effectively penetrates the entire depth of the film. The filling fraction is as high as 60–70% for films with thickness $< 3 \mu\text{m}$; however, as the film thickness increases, the filling fraction goes down, which may be the cause of poor efficiency of thick ss-DSCs. We have used a lower spin coating speed and higher spiro-OMeTAD solution concentration to increase the filling fraction and consequently the efficiency of ss-DSCs. Development of $>10\%$ efficient ss-DSCs will most likely require $>5\text{-}\mu\text{m}$ -thick TiO_2 films, and such significant increase in thickness will require

both reduction in recombination and improvement in pore filling. XPS depth profiling and absorption spectroscopy will be necessary when evaluating future HTMs and new pore filling schemes. Further improvement in the filling fraction can be expected by reducing the evaporation speed of solvent during spin coating, or switching from spin coating to other pore filling methods such as micropipetting^[17] or melt infiltration.^[28]

4. Experimental

Sample Preparation: The standard ss-DSC sample preparation method has been published elsewhere [18]. To summarize, the TiO_2 films were deposited on FTO substrate ($15 \Omega \text{ cm}^{-1}$, Pilkington) patterned through etching with zinc powder and HCl (4N) to give the required electrode. The FTO was pre-treated with a 0.02 M aqueous TiCl_4 at 60°C for 6 hours. Samples used for efficiency measurements were coated with a compact layer of TiO_2 (100 nm) by aerosol spray pyrolysis deposition at 450°C using oxygen as the carrier gas [29,30]. Mesoporous TiO_2 films for XPS depth profiling were fabricated by doctor-blading TiO_2 paste from Solaronix SA (Ti-Nanoxide T series); films for pore filling and efficiency measurements were screen-printed with a homemade TiO_2 paste [15]. These sheets were then slowly heated to 500°C (ramped over 30 min) and baked at this temperature for 30 min under an oxygen flow.

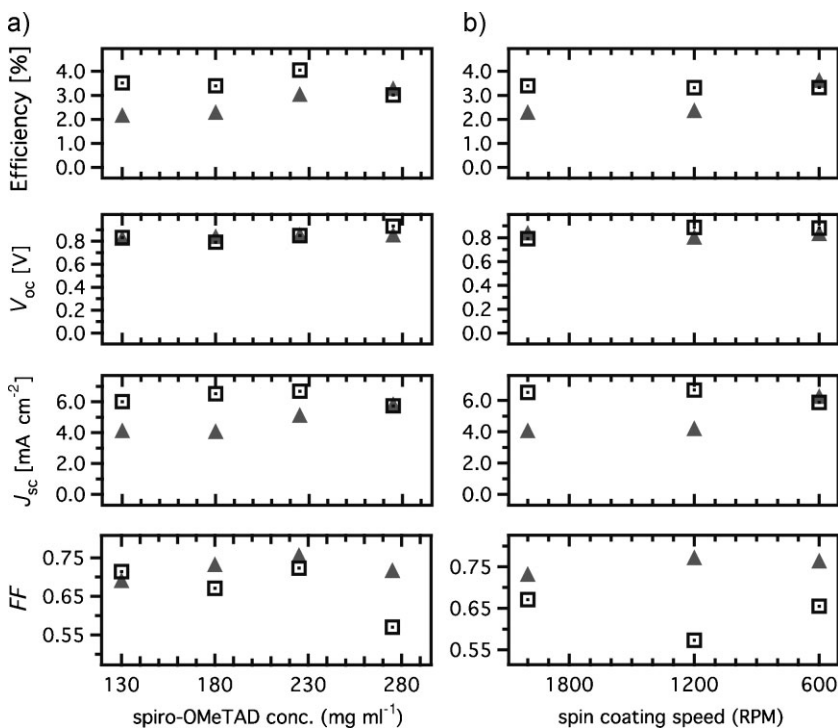


Figure 5. Power conversion efficiency, V_{oc} , J_{sc} and fill factor (FF) for ss-DSCs versus a) spiro-OMeTAD concentration in chlorobenzene and b) spin coating speed. Outlined squares and filled triangles are for 2.4- μm - and 3.0- μm -thick TiO_2 films, respectively.

Acidic TiCl_4 treatment was repeated before slowly reheating (ramped over 30 minutes) to 450 °C and baking at this temperature for 30 minutes with subsequent cooling to 80 °C. For depth profiling and pore filling measurements, the mesoporous TiO_2 electrodes were placed for 18 hours in a pure Z907 dye solution, which comprised 3 mM of Z907 (Solaronix SA) in 1:1 mixture of acetonitrile and *tert*-butyl alcohol. For efficiency measurements, the electrodes were placed for 10 minutes in a 6 mM Z907 and 4-guanidinobutyric acid (GBA, Fluka) as coabsorbent in a 1:1 mixture in 1-methoxy-2-propanol solution (98+%, Aldrich) [31]. The dye-coated mesoporous films were briefly rinsed in acetonitrile and dried in air for one minute.

Spiro-OMeTAD Infiltration: Spiro-OMeTAD (EMD Chemicals; Merck GmbH) was completely dissolved in chlorobenzene by heating and stirring the solution at 70 °C for 30 minutes. For efficiency measurements, *tert*-butyl pyridine (tbp) was added to the solution with a volume to mass ratio of 1:26 $\mu\text{L mg}^{-1}$ *tbp*:spiro-OMeTAD. Lithium bis(trifluoromethylsulfonyl)imide salt (Li-TFSI) ionic dopant was pre-dissolved in acetonitrile at 170 mg mL^{-1} , then added to the HTM solution at 1:12 $\mu\text{L mg}^{-1}$ of Li-TFSI solution:spiro-OMeTAD. Upon changing the concentration of spiro-OMeTAD in the solution, the ratio of spiro-OMeTAD to *tbp* and Li-TFSI was kept constant.

A small quantity (10–70 μL) of the spiro-OMeTAD solution was deposited onto each TiO_2 film (area = 0.20–0.28 cm^2) at room temperature and left for 1 minute before spin coating at 2000 RPM for 45 s in nitrogen atmosphere. After spin coating, the film was dried overnight at room temperature in air.

XPS Depth Profiling: XPS spectra were acquired with a PHI 5000 Versaprobe system using a microfocused (100 μm , 25 W) Al K_{α} X-ray beam with a photoelectron takeoff angle of 45°. A dual-beam charge neutralizer (10 V Ar^+ and 30 V electron beam) was used to compensate the charge-up effect. Ar^+ ion source was operated at 1 nA and 5 kV, with rastering on an area of 1 mm \times 1 mm. In order to calculate the sputter rate, the film thicknesses were measured with a Dektak 150 surface profiler. The sputter rate was around 25 nm min^{-1} for all spiro-OMeTAD infiltrated mesoporous TiO_2 films.

Absorption Spectroscopy: After spiro-OMeTAD infiltration, we used a chlorobenzene-soaked cotton swab to remove the excess spiro-OMeTAD on the substrate that was not on top of the mesoporous TiO_2 film. The spiro-OMeTAD overlayer thickness was measured by imaging the cross-section of the film with scanning electron microscopy (FEI XL30 Sirion SEM) operated at an accelerating voltage of 5 kV. After the overlayer thickness measurement, the sample was immersed in chlorobenzene for one hour at room temperature. To ensure the accuracy of absorption measurement, the solution was subsequently diluted to tune the optical density between 0.1 and 1.0 at 389 nm. The absorption measurement was carried out in Cary 6000i UV–vis–NIR spectrophotometer.

Back Contact and Photovoltaic Measurements: For efficiency measurements, the counter electrode was applied by thermal evaporation of 100 nm of gold. FTO glass plates (Nippon Sheet Glass, Solar, 4-mm thick) were cleaned in a detergent solution using an ultrasonic bath for 15 min. The power of an AM 1.5 solar simulator equipped with a Xe-lamp was calibrated using a reference Si photodiode equipped with an IR cut-off filter (KG-3, Schott) in order to reduce the mismatch in the region of 350–750 nm between the simulated light and AM 1.5 to less than 2% [32,33].

Acknowledgements

This publication was partially based on work supported the Center for Advanced Molecular Photovoltaics (Award No KUS-C1-015-21), made by King Abdullah University of Science and Technology (KAUST). It was also partially supported by the Office of Naval Research. I-K. Ding is supported by a Chevron Stanford Graduate Fellowship. We thank Chuck Hitzman and Dr. Michael Kelly for valuable discussions and experimental assistance with X-ray photoelectron spectroscopy and Dr. Brian O'Regan for giving us the idea of dissolving out spiro-OMeTAD from the pores. Jérémie Brillat received financial support from a Marie Curie Research Training Network, Hydrogen Project (MRTN-CT-2006-032474). Supporting Information is available online from Wiley InterScience or the author.

- [1] Y. Chiba, A. Islam, Y. Watanabe, R. Komiya, N. Koide, L. Han, *Jpn. J. Appl. Phys., Part 2* **2006**, 45, L638.
- [2] F. Gao, Y. Wang, D. Shi, J. Zhang, M. Wang, X. Jing, R. Humphry-Baker, P. Wang, S. M. Zakeeruddin, M. Grätzel, *J. Am. Chem. Soc.* **2008**, 130, 10720.
- [3] M. Grätzel, *Prog. Photovoltaics* **2006**, 14, 429.
- [4] H. J. Snaith, L. Schmidt-Mende, *Adv. Mater.* **2007**, 19, 3187.
- [5] U. Bach, D. Lupo, P. Comte, J. E. Moser, F. Weissortel, J. Salbeck, H. Spreitzer, M. Grätzel, *Nature* **1998**, 395, 583.
- [6] H. J. Snaith, A. J. Moule, C. Klein, K. Meerholz, R. H. Friend, M. Grätzel, *Nano Lett.* **2007**, 7, 3372.
- [7] L. Schmidt-Mende, S. M. Zakeeruddin, M. Grätzel, *Appl. Phys. Lett.* **2005**, 86, 013504.
- [8] F. Fabregat-Santiago, J. Bisquert, L. Cevey, P. Chen, M. Wang, S. M. Zakeeruddin, M. Grätzel, *J. Am. Chem. Soc.* **2009**, 131, 558.
- [9] J. R. Jennings, L. M. Peter, *J. Phys. Chem. C* **2007**, 111, 16100.
- [10] J. Kruger, R. Plass, M. Grätzel, P. J. Cameron, L. M. Peter, *J. Phys. Chem. B* **2003**, 107, 7536.
- [11] H. J. Snaith, M. Grätzel, *Adv. Mater.* **2007**, 19, 3643.
- [12] L. Schmidt-Mende, M. Grätzel, *Thin Solid Films* **2006**, 500, 296.
- [13] J. E. Kroeze, N. Hirata, L. Schmidt-Mende, C. Orizu, S. D. Ogiev, K. Carr, M. Grätzel, J. R. Durrant, *Adv. Funct. Mater.* **2006**, 16, 1832.
- [14] U. Bach, *Ph.D. Thesis*, École Polytechnique Fédérale de Lausanne, Switzerland **2000**.
- [15] C. J. Barbe, F. Arendse, P. Comte, M. Jirousek, F. Lenzmann, V. Shklover, M. Grätzel, *J. Am. Ceram. Soc.* **1997**, 80, 3157.
- [16] N. Fukuri, N. Masaki, T. Kitamura, Y. Wada, S. Yanagida, *J. Phys. Chem. B* **2006**, 110, 25251.
- [17] B. O'Regan, F. Lenzmann, R. Muis, J. Wienke, *Chem. Mater.* **2002**, 14, 5023.
- [18] H. J. Snaith, R. Humphry-Baker, P. Chen, I. Cesar, S. M. Zakeeruddin, M. Grätzel, *Nanotechnology* **2008**, 19, 424003.
- [19] H. W. Han, U. Bach, Y. B. Cheng, R. A. Caruso, *Appl. Phys. Lett.* **2007**, 90, 213510.
- [20] J. J. Blackstock, C. L. Donley, W. F. Stickley, D. A. A. Ohlberg, J. J. Yang, D. R. Stewart, R. S. Williams, *J. Am. Chem. Soc.* **2008**, 130, 4041.
- [21] *ToF-SIMS: Surface Analysis by Mass Spectrometry* (Eds. J. C. Vickerman, D. Briggs), IM Publications, West Sussex **2001**.
- [22] K. M. Coakley, Y. Liu, M. D. McGehee, K. L. Frindell, G. D. Stucky, *Adv. Funct. Mater.* **2003**, 13, 301.
- [23] J. W. Park, S. S. Park, Y. Kim, I. Kim, C. S. Ha, *ACS Nano* **2008**, 2, 1137.
- [24] N. Papageorgiou, C. Barbe, M. Grätzel, *J. Phys. Chem. B* **1998**, 102, 4156.
- [25] H. J. Snaith, L. Schmidt-Mende, M. Grätzel, *Phys. Rev. B* **2006**, 74, 045306.
- [26] F. Fabregat-Santiago, J. Bisquert, E. Palomares, L. Otero, D. Kuang, S. M. Zakeeruddin, M. Grätzel, *J. Phys. Chem. C* **2007**, 111, 6550.
- [27] E. Palomares, J. N. Clifford, S. A. Haque, T. Lutz, J. R. Durrant, *J. Am. Chem. Soc.* **2003**, 125, 475.
- [28] K. Fredin, E. M. J. Johansson, T. Blom, M. Hedlund, S. Plogmaker, H. Siegbahn, K. Leifer, H. Rensmo, *Synth. Met.* **2009**, 159, 166.
- [29] L. Kavan, M. Grätzel, *Electrochim. Acta* **1995**, 40, 643.
- [30] H. J. Snaith, M. Grätzel, *Adv. Mater.* **2006**, 18, 1910.
- [31] Z. Zhang, S. M. Zakeeruddin, B. C. O'Regan, R. Humphry-Baker, M. Grätzel, *J. Phys. Chem. B* **2005**, 109, 21818.
- [32] M. K. Nazeeruddin, P. Pechy, T. Renouard, S. M. Zakeeruddin, R. Humphry-Baker, P. Comte, P. Liska, L. Cevey, E. Costa, V. Shklover, L. Spiccia, G. B. Deacon, C. A. Bignozzi, M. Grätzel, *J. Am. Chem. Soc.* **2001**, 123, 1613.
- [33] S. Ito, H. Matsui, K. Okada, S. Kusano, T. Kitamura, Y. Wada, S. Yanagida, *Sol. Energy Mater. Sol. Cells* **2004**, 82, 421.